Temperature dependent Characteristics of the JPL Silicon MEMS Gyroscope.

Kirill Shcheglov, Christopher Evans, Roman Gutierrez, and Tony K. Tang,
Jet Propulsion Laboratory, California Institute of Technology,
4800 Oak Grove Dr. , Pasadena, CA 91109
(818) 354-2222
email: kvs@mail1.jpl.nasa.gov

Abstract

Advances in aeronautics and space technology have created a need for miniaturized navigation instruments such as gyroscopes, a need which is currently being addressed by a number of micromachined designs. While micromachined devices have already proven their advantages being light-weight and low-power, the performance limitations of these devices have not been thoroughly investigated. In particular the effects of the temperature environment on the performance is of great interest since they can be a dominant source of error in micromachined devices. We have investigated the temperature–dependent drift and noise characteristics of a packaged silicon MEMS gyroscopes with and without the micromachined thermal isolation. Packaged devices were subjected to various temperatures environments between –60 and +60 °C, and their resonant frequencies, signal drifts and quadrature drifts were monitored. The results obtained from these tests point out the mechanisms of temperature-dependent and temperature-independent drift and suggest a scheme for temperature compensation. These results will be compared with a theoretical model for temperature effects. Theoretically achievable performance limits of this class of MEMS devices are discussed.

TABLE OF CONTENTS

1. INTRODUCTION

In order for a gyroscope to be considered useful for a real application a number of tests must be done. These include the basic performance and noise characteristics, reliability, effects of vibration and shock, of radiation is a space application is contemplated, and of temperature. The last is especially important for spacecraft applications where the temperature may fluctuate by over 100 °C, depending on spacecraft design, instrument position within the spacecraft, and the spacecraft orientation relative to the sun. In the following paper temperature testing done on a silicon micromachined gyroscope developed at JPL will be described.

2. DEVICE DESCRIPTION

The JPL silicon micromachined gyroscope is a vibratory gyroscope manufactured out of silicon using bulk micromachining techniques[1]. The basic design (Fig. 1) consists of a silicon cloverleaf structure supported by four springs and a vertical post through the center of the cloverleaf. The while structure vibrates in one rocking mode (drive mode).

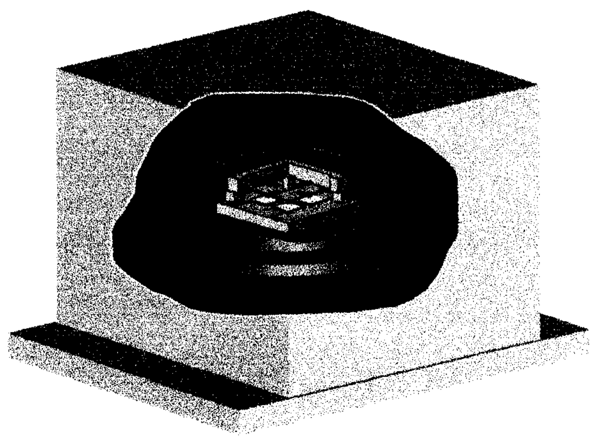

Figure 1. Schematic of the JPL micromachined vibratory gyroscope.

Rotation, through Coriolis force, couples energy into the a nearly degenerate orthogonal rocking mode (sense mode). The motion in the sense mode is detected capacitively with a trans-impedance circuit. In this structure the post is the inertial sensing element, and the leaves are used for electrostatic excitation and capacitive sensing. This structure is packaged in an evacuated metal can which in turn is enclosed in an aluminum box with some preamplifier electronics. The bulk of the control and signal processing electronics is housed in a separate package.

3. TESTING SETUP

The temperature tests were done on a packaged gyro at rest (no rotation) under varying temperature conditions. The gyro box was placed inside a temperature testing chamber (Scionics BTC-710-3) and the following gyro outputs were monitored by a computer with custom testing software:

Analog rate signal: This is the actual gyroscope output. This signal was used to generate Green charts at various constant temperatures as well as to measure temperature-dependent drift during temperature ramps.

Quadrature signal: This signal is the gyro output demodulated in quadrature (90° to the analog rate output). This signal is indicative of relative mode drifts and modeshape changes.

Package temperature: the temperature was measured with a platinum resistor inside the aluminum box. Although the resistor was in close proximity to the gyro can, the gyro temperature lagged the package temperature by about 3-5 min, as can be seen from the data. A more immediate (although uncalibrated) measure of the actual device temperature can be obtained from tracking the gyro resonant frequency.

Gyro resonant frequency: gyro drive signal tapped from the drive feedback loop measured with a frequency counter (HP 53131A). The frequency is a good indication of the instantaneous device temperature.

AGC voltage: the amplitude of the gyro drive signal. It is a measure of the Q-factor of the gyro resonator.

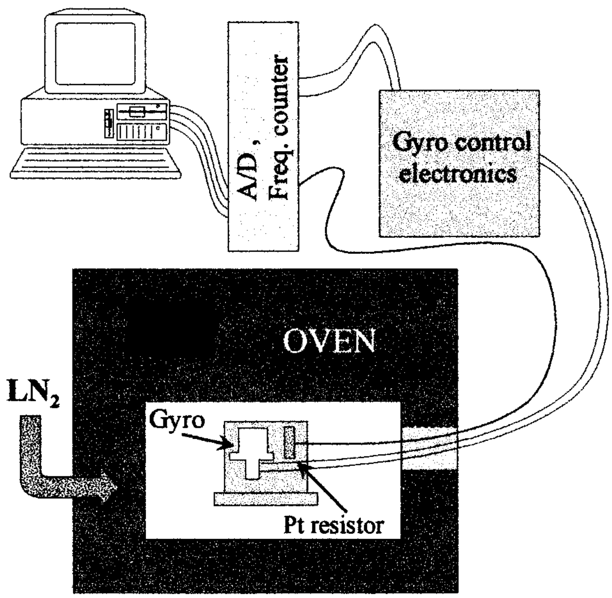

Figure 2. Schematic of the gyro testing setup.

Two sets of tests were performed on the gyro. In the first set, the oven temperature was set to a constant value and maintained there throughout the test while the gyro signal was monitored. Allen variance plots were thus produced at a number of temperatures between –60 and +60 °C. In addition, correlations between bias drift and small temperature fuctuations were recorded. In the second set of tests the temperature was ramped between –60 and +60 °C and various gyro outputs described above were recorded.

4. TEST RESULTS

Constant temperature tests.

Figure 3a shows the signal and the quadrature plot taken at -60 C. Figure 3b shows the temperature and the frequency plots during the same test, and 3c - the signals in 3a plotted vs. frequency. Since the frequency can be taken as a good. measure of device temperature (this will be further motivated

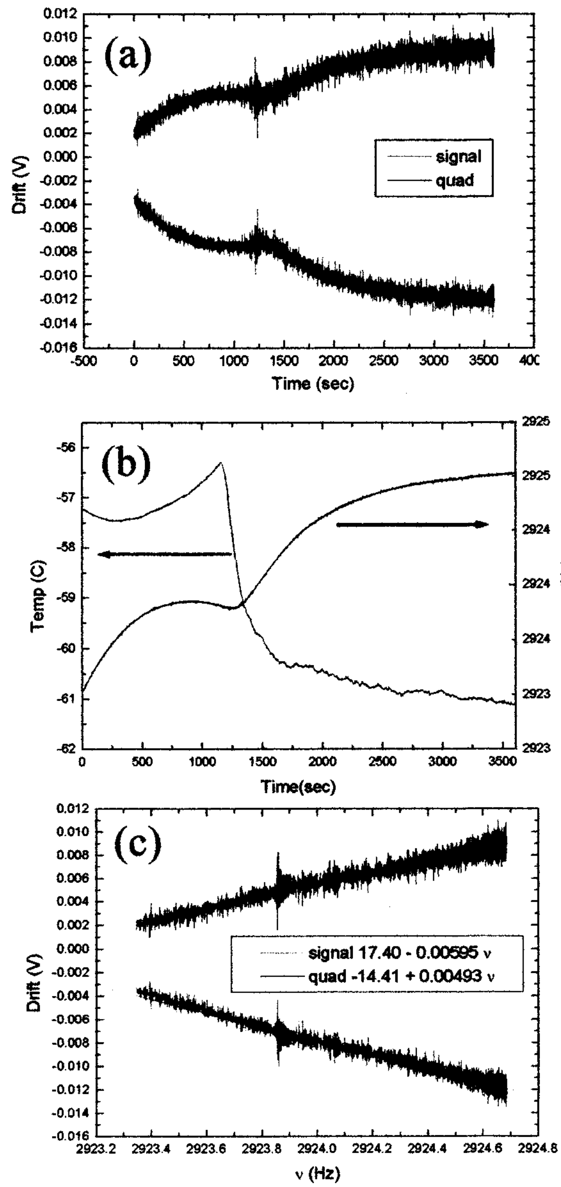

Figure 3. Temperature test at -60 °C: (a) rate signal and quadrature vs. time; (b) temperature and frequency vs. time; (c) rate signal and quadrature vs. frequency.

-40 ℃

-20 ℃

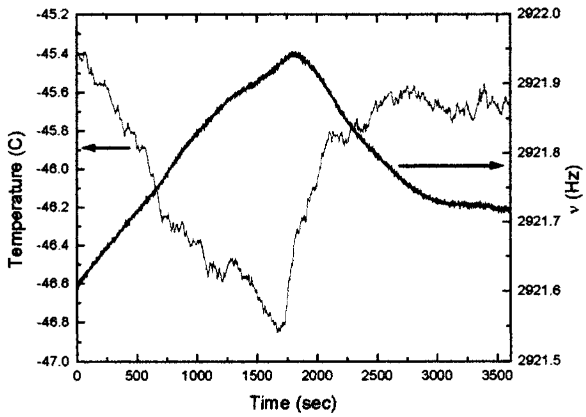
Temperature (C)
ν (Hz)
Time (sec)

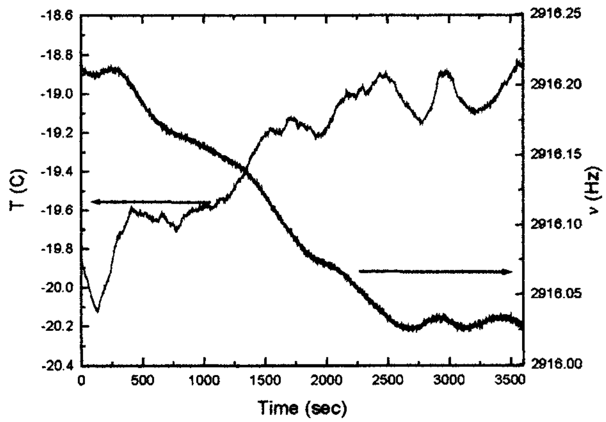
T (C)
ν (Hz)
Time (sec)

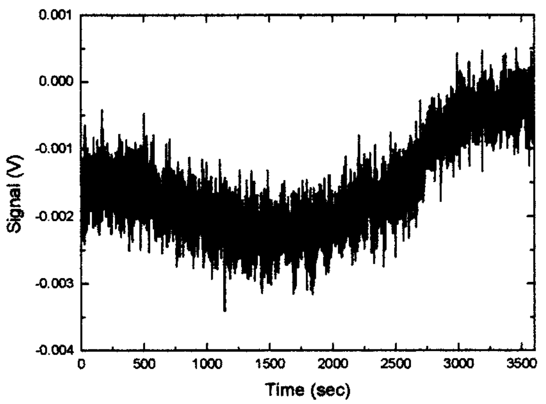
Signal (V)
Time (sec)

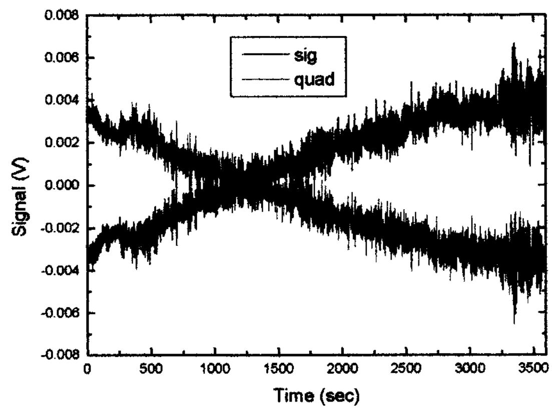
sig
quad
Signal (V)
Time (sec)

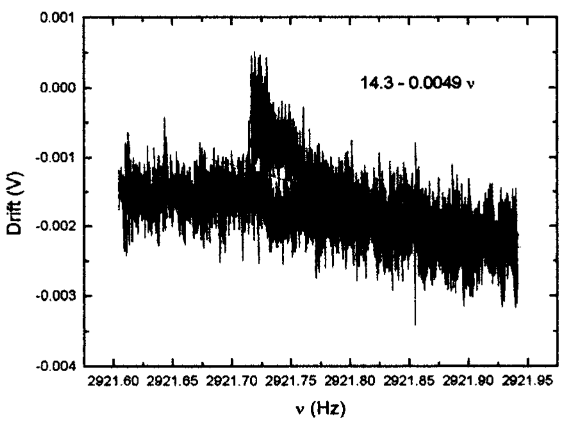
14.3 - 0.0049 ν
Drift (V)
ν (Hz)

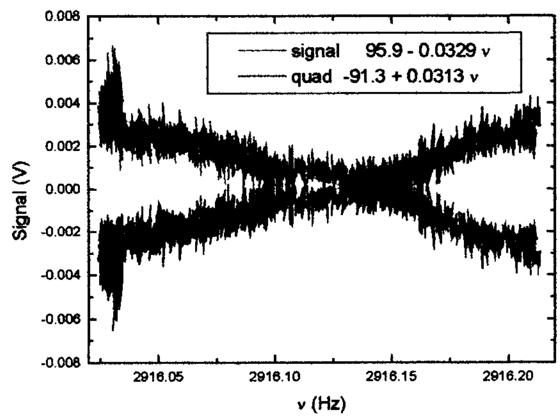
signal 95.9 - 0.0329 ν
quad -91.3 + 0.0313 ν
Signal (V)
ν (Hz)

0 °C

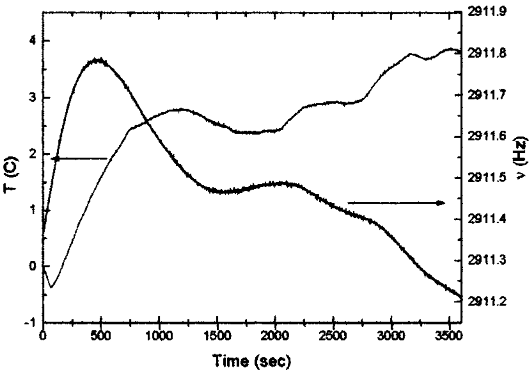
T (C)
ν (Hz)
Time (sec)

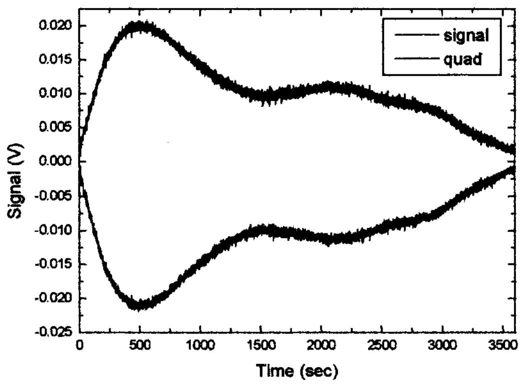
signal
quad
Signal (V)
Time (sec)

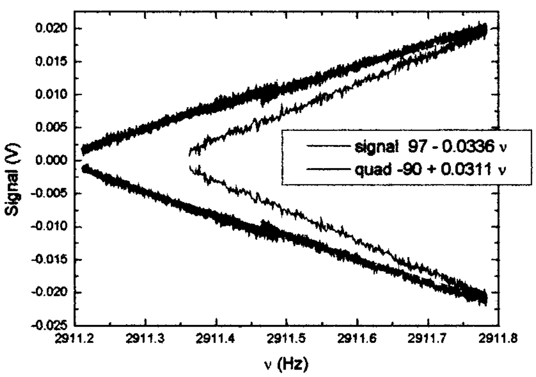
signal 97 - 0.0336 ν
quad -90 + 0.0311 ν
Signal (V)
ν (Hz)

20 °C

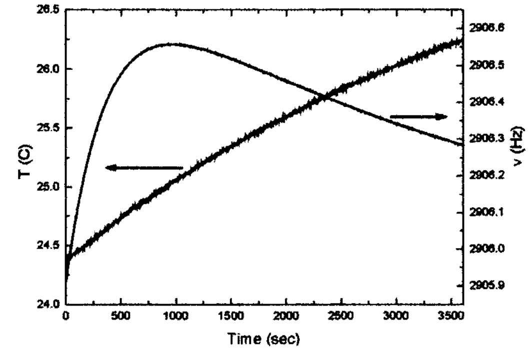
T (C)
ν (Hz)
Time (sec)

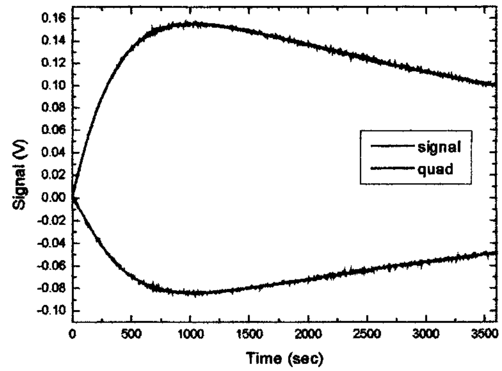
signal
quad
Signal (V)
Time (sec)

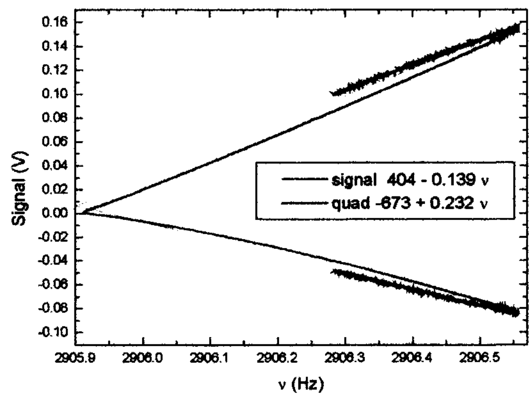
signal 404 - 0.139 ν
quad -673 + 0.232 ν
Signal (V)
ν (Hz)

40 ℃

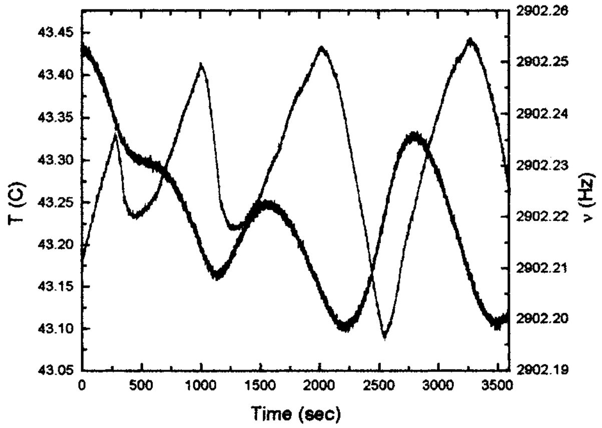
T (C)
ν (Hz)
Time (sec)

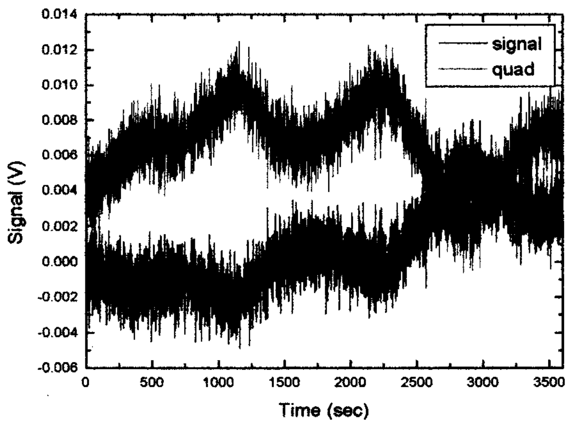
signal
quad
Signal (V)
Time (sec)

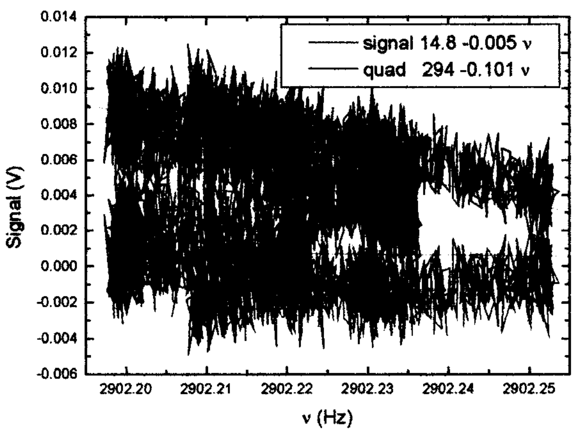
signal 14.8 -0.005 ν
quad 294 -0.101 ν
Signal (V)
ν (Hz)

60 ℃

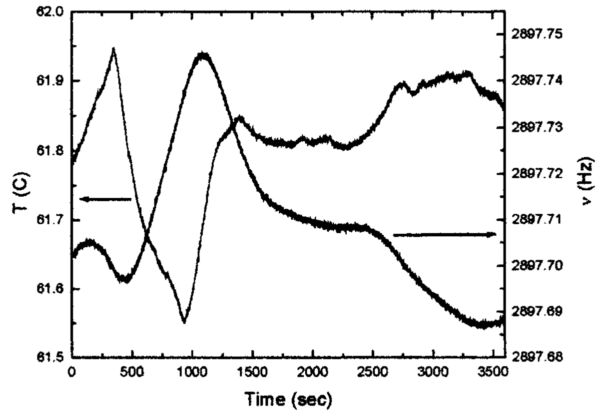
T (C)
ν (Hz)
Time (sec)

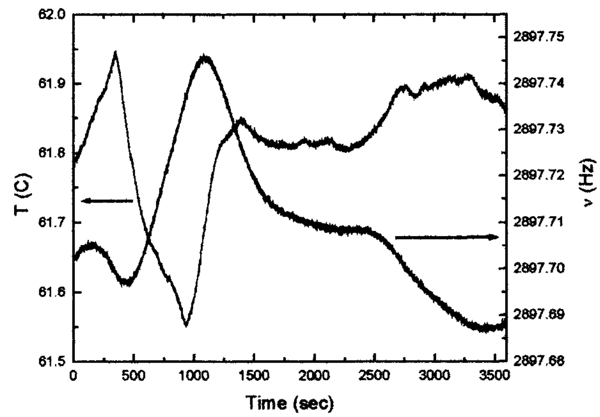
T (C)
ν (Hz)
Time (sec)

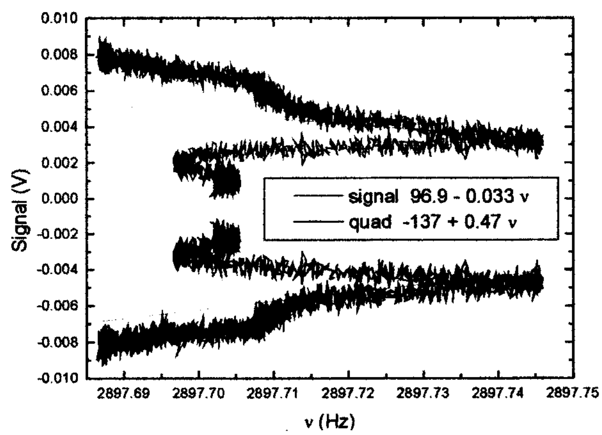
signal 96.9 - 0.033 ν
quad -137 + 0.47 ν
Signal (V)
ν (Hz)

when temperature ramp tests are discussed.) It is evident that at this temperature small signal drifts track small temperature fluctuations quite precisely. Following Fig. 3 are the results for other temperatures up to + 60 °C. The same picture is observed for temperatures up to 0 °C. At higher temperatures this is no longer holds true. Another source of the signal drift appears and begins to dominate at higher temperatures. This effect will be seen to originate from changes in the resonator Q.

The plots in Fig. 4 summarize the results of the constant temperature 1 hr long runs. Here the Green chart minimum is calculated using the responsivity of 14mV/(deg/sec) measured in earlier tests.

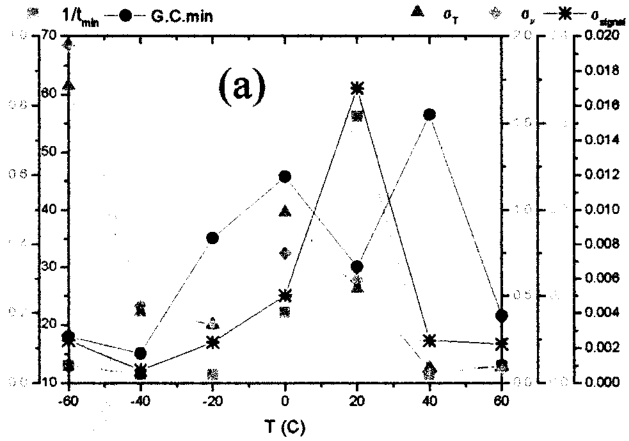

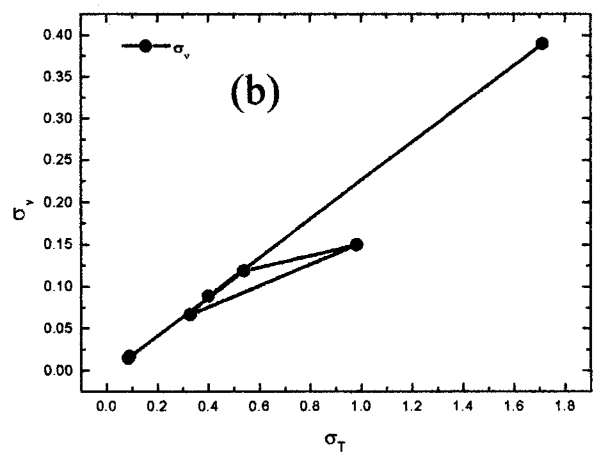

Figure 4. (a) Summary of constant temperature tests; (b) An excellent correlation between σ_T and σ_v is observed.

One notable correlation is observed: the standard deviation of the frequency very closely tracks that of temperature. Thus the gyro resonant frequency can be used as an instantaneous measure of the device temperature. This is also observed in the temperature ramp tests discussed later. The dependence of the resonant frequency on temperature is most likely due to the thermal expansion coefficient mismatch between the gyro structure an the package. Shown below (Fig. 5) is the simulated "pure" temperature dependence of the gyro frequency – i.e. the temperature dependence of the elastic constants take from literature [2] + inertia changes from thermal expansion compared with the observed temperature dependence of the frequency. The sensitivity to temperature is a factor of 3 larger than that predicted from pure elastic considerations. This indicates that the dominant mechanism for temperature dependence is external to the silicon gyro core and most likely is caused by temperature-induced stresses in the package.

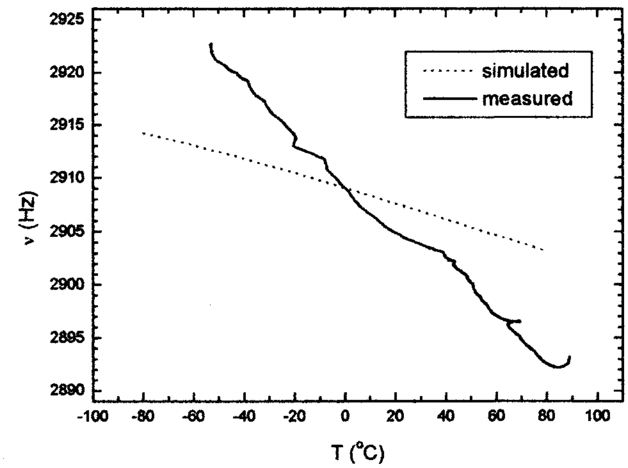

Figure 5. Comparison of simulated and measured frequency dependence on temperature.

We observe also, that in general the performance of the gyro can be rather high with decent temperature control (within about a degree) below about 20 °C. An on-chip Pt resistor can be used to measure the temperature of the gyro directly and the drift can be further reduced by compensating for the small temperature fluctuations in software. In absence of this on-chip resistor, the gyro frequency can be used as the measure of the device temperature with some preliminary calibration.

Above 20 C other noise sources seem to dominate the temperature fluctuations. The most probable candidates seem to be electrostatic coupling of the drive signal and low-frequency noise in the AGC loop. This will be seen more clearly from the temperature ramp tests that will be discussed below.

Temperature ramp tests

The plots in Figure 6 show the frequency dependence on temperature between –60 and +60 °C. The frequency tracks the temperature quite nicely (there is an about 5 min delay between the features; this time-lag is the time it takes for the heat to get from the package to the gyro device inside). This indicates that for devices without the internal Pt resistor for direct temperature measurement, the gyro frequency can be used as an indication of the device temperature with appropriate calibration. The results of frequency vs temp. fits for different ramp tests are in rather good agreement. They are summarized in Table 1

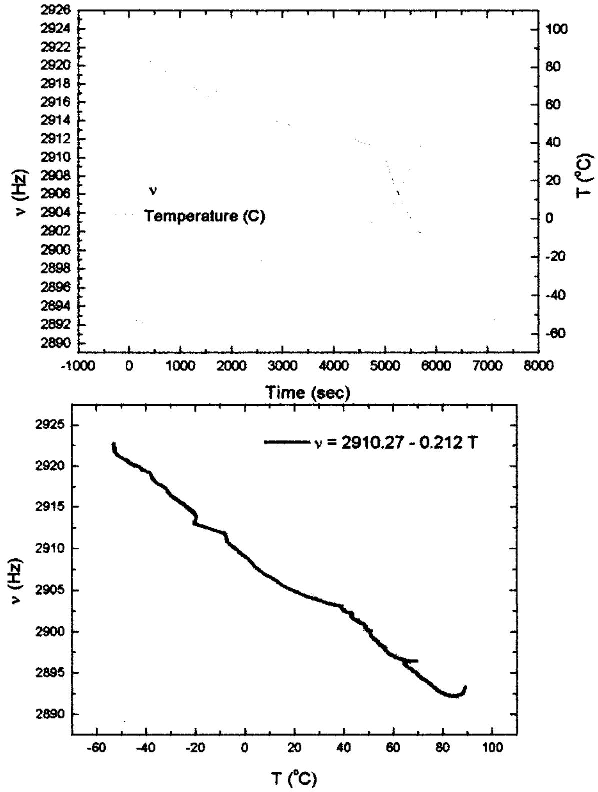

Figure 6. Dependence of frequency on temperature and a linear fit to the data.

Test	ν(T)
20 °C – 40 °C	2913.06 – 0.260 T
0 °C – 60 °C	2913.68 – 0.232 T
-60 °C – 60 °C	2914.73 – 0.221 T
60 °C – -60 °C	2910.27 – 0.212 T
-80 °C – 40 °C	2913.13 – 0.214 T

Table 1. Summary of frequency vs. T results for different ramp tests.

The results match to within about 10%. This indicates that frequency can be used to correct for the drift due to small fluctuations in temperature (1-2 degrees) around a set-point and lower the noise by about a factor of 10.

Figure 7 shows the results of a temperature ramp test. Although the frequency decreases monotonically as the temperature increases, the rate signal and quadrature signal exhibit non-monotonic behavior. In the next test in order to investigate this behavior, the AGC voltage was monitored as well.

Figure 8 shows the dependence of the AGC voltage on temperature. The sharp rise in the AGC voltage around 10-15 °C indicates a sharp degradation in the Q-factor of the resonator.

This degradation is responsible for the generally higher noise at high temperatures in two ways:

1. The increase in the intrinsic resonator noise (random walk).
2. Coupling of the low frequency AGC loop noise through the gyro drive signal.

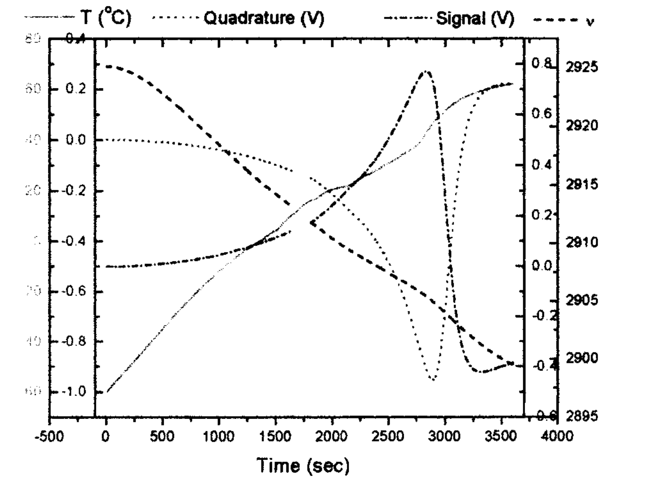

Figure 7. Various gyro outputs during the temperature ramp test.

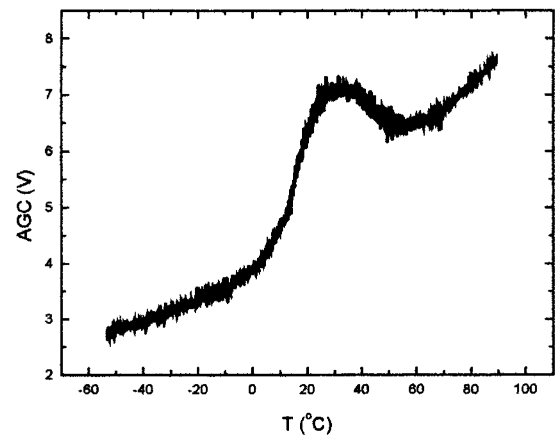

Figure 8. Dependence of the AGC voltage on temperature.

In general large signal drifts at higher temperatures that do not track the frequency of the gyro seem to be associated with the changes in the AGC voltage. This large degradation in Q is most likely due to outgasing either from the gyro package walls or from the getter inside the gyro can. Water is a likely candidate since this outgasing happens around 20 °C. Baking the gyro package for longer periods of time prior to packaging could reduce this effect significantly.

Shown in Figure 9 is a plot of the frequency, signal and AGC voltage. Here the signal is in deg/hr using the responsivity of 118 mV/deg/sec. The two sources of drift are clearly evident. The signal is affected by the frequency as well as by the AGC voltage.

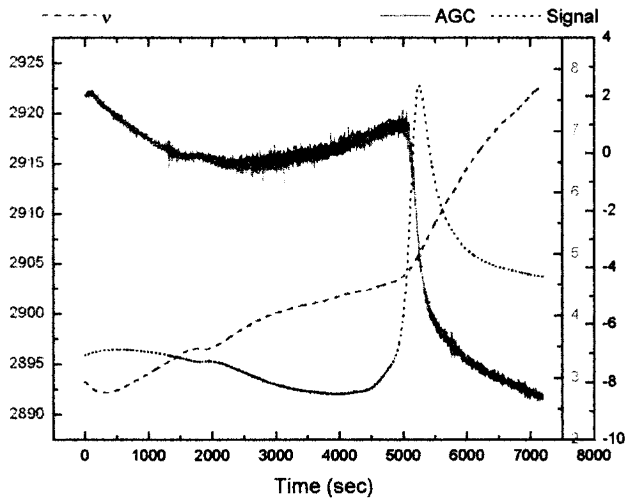

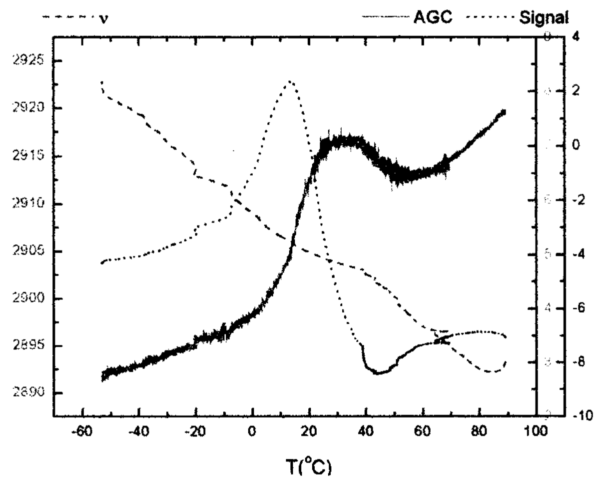

Figure 9. Plots of frequency, signal, and AGC voltage vs. time and vs. temperature. The two sources of drift are clearly visible.

Summary of ramp test results.

The Temperature Ramp testing has revealed two significant
1. The frequency changes linearly with temperature. The magnitude if the scale factor is about 3 times that predicted from purely elastic considerations and caused by dissimilar expansion coefficients of different materials comprising the gyro package.
The new gyro design has an extra suspension isolating the silicon gyro core from the outside frame. This suspension is expected to significantly reduce the thermally induced stresses associated with the gyro can expansion.
2. A significant degradation of the resonator Q occurs at about 15 °C. This degradation strongly influences the drift an contributes to the noise of the gyro. Also, this degradation is the reason why the drift does not track small temperature fluctuations above 20 °C. The solution of this problem is an improved gyro package and a more thorough bakeout of all the components prior to packaging. A getter change may also be needed if the gyro is expected to operate will at elevated temperature.

5. CONCLUSIONS

Summary of results.

A number of important results were evident from the temperature tests:

1. Temperature fluctuations are a major source of low frequency noise (drift). The temperature affects the gyro in two ways through changes in gyro resonant frequency and through changes in the resonator Q and thus the drive amplitude.
Thus, to achieve high sensitivity operation the temperature must be controlled. In addition, small fluctuations (on the order of 0.1-1 degree) must also be accounted for.

2. Frequency depends linearly on temperature. Thus, with some calibration, the frequency can be measured and used as a gauge of the gyro device temperature.

3. Above 20 °C the Q factor of the sealed resonator degrades significantly as seen from the AGC voltage vs. T plots. This is most likely a packaging problem. Gyro packages must be baked out in vacuum before use. It appears that above 30C the major source of drift is the significant increase of the AGC voltage and through it of electrical noise from the AGC loop.
Also, mechanically coupled vibration from the fan inside the temperature chamber appears as noise on the AGC voltage.

Solutions and future work.

1. The new gyro design contains an extra suspension isolating the gyro core from the outside frame which is attached to the package. This suspension will improve the performance in two ways.
a. it will smooth out external temperature fluctuations.
b. It will isolate the gyro core from stresses induced by thermal expansion mismatch between the gyro silicon and the package material, and thus will reduce the frequency dependence on temperature by about a factor of three. The remaining frequency dependence is intrinsic to the silicon and can not be removed. It can, however, be compensated for with an internal temperature measurement, such as an integrated Pt resistor on the gyro baseplate, or, in absence of such, the gyro frequency itself can be taken, with some calibration, as a measure of the device temperature.
The significant degradation of the resonator Q at higher temperatures is a cause for worry. The packaging of the gyro must be improved to overcome this problem. The gyro and the package must be baked out thoroughly prior to packaging, and the getter may have to be changed to one that outgases at higher temperature.

In conclusion, the temperature effects on the gyro performance were quantified and identified. Analysis of results suggested a number of improvements which are being implemented in the new gyro design.

With the present device (without improvement mentioned above) for low-noise operation the best solution would be a temperature-controlled environment below 20 °C with an internal temperature gauge used to correct for small temperature fluctuations. However, simulations show that even with improvements such as stress isolation, internal temperature of the device must be monitored so that small fluctuations can be compensated for.

6. ACKNOWLEDGEMENTS

The materials in this paper were prepared by the Center for Space Microelectronics Technology, Jet Propulsion Laboratory, California Institute of Technology, and were sponsored by the National Aeronautics and Space Administration, Office of Space Science.

7. REFERENCES

[1] T.K.Tang, R.C.Gutierrez, J. Wilcox, C. Stell, V. Vorperian, R. Calvet, W. Li, I. Charkaborty, R. Bartman, W. Kaiser, "Silicon Bulk Micromachined Vibratory Gyroscope", Tech Digest, Solid-State Sensor and Actuator Workshop, Hilton Head, S.C. pp.288-293, June 1996.

[2] O. Madelung, *Semiconductors. Group IV elements and III-V compound*, Springer-Verlag, New York, 1991.